

Formation optimization tool for AUV-based seismic surveys

Sérgio M. Jesus

LARSyS, University of Algarve, Campus de Gambelas
8005-139 Faro, Portugal
Email: sjesus@ualg.pt

Abstract—This paper presents a tool for determining the optimal formation of a swarm of Autonomous Underwater Vehicles (AUV) for seismic surveying. Each AUV carries an acoustic streamer so, the AUV formation implies a space distributed sensor array for bottom imaging. This tool is based on a sparse formulation of bottom layer reflection resulting on a structured design matrix with the bottom return field. Since the design matrix structure depends also on the receiving system characteristics, field coherence is used as optimization criteria for determining sensor array position and thus the vehicle formation. The receiver positions are constrained by actual array characteristics and AUV relative position physical constraints. Simulated results based on actual physical propagation model data are provided for a two sparker source and four AUV 2D geometry case in the scenario of the port of Sines (Portugal). The results show that a clear improvement can be reached regarding bottom layer resolution for a 3D bottom model. The developed methodology may be useful for resource planning and setup of seismic surveying experiments involving moving sensing arrays such as those under test in the EU H2020 WiMUST project¹.

I. INTRODUCTION

The concept developed under project WiMUST¹, involving a swarm of autonomous surface and underwater vehicles (ASV & AUV) for sub-bottom profiling, is a game changer in the seismic community. The proposed idea is disruptive at two levels: at the system hardware level by introducing the concept of autonomous robotics for seismic surveying, and at the seismic data processing software level by allowing for on the fly configurable distributed sensor arrays (DSA) for sub-bottom estimation. These two levels of abstraction - hardware and software - are closely intertwined and interdependent.

The system hardware encompasses both ASV and AUV, carrying seismic sources and acoustic streamers, respectively. Scientific and technological challenges are, among others, those dealing with vehicle coordination, navigation, positioning, communication and synchronization are dealt with separately, while the interest will be focused on the processing of the acoustic data for sub-bottom estimation purposes.

Seismic data processing has become a relatively standard task, for which there are very complete and high performance software packages both proprietary and public (open source). This standardization was made possible thanks to maintaining constant some basic assumptions throughout the sensing system configuration, the source-receiver time-space synchronization and the data flow. Under this concept, if one wants to take full advantage of the system spatial reconfiguration

capabilities, one or more of these basic assumptions may be violated. Reconfiguration in this case means that source-receiver positions may change through time and adopt (almost) any geometry. The crucial question is how to determine the best suited geometry and, in case, how does this geometry should change during the survey. The ability to navigate and individually control seismic sources and acoustic receivers along range, cross-range and depth allows to design seismic systems that may take, at least conceptually, any spatial shape. As in many other similar problems, determining the most suited (or optimal) source - receiver positioning is ill-posed, computationally cumbersome and non-linear since it is, itself, dependent on the quantity to be estimated: the bottom properties.

An approach to answer this question was based on the low acoustic field coherence criteria, proposed and tested with simulated data [1]. Building on these results, the practical Formation Optimization Tool (FOT), aimed at survey planning and performance prediction, has been developed and is described herein. FOT extends the capabilities of previously shown 2D results to 3D scenarios and range-dependent environments. The results shown herein cover the preparation of WiMUST sea trials Sines'17 in the port of Sines (Portugal)

II. BACKGROUND ON OPTIMALITY

A. Numerical modeling

The acoustic received field at observation location \mathbf{r}_k due to a unit amplitude monochromatic point source located at \mathbf{r}_s may be written using the Green function $G(\cdot)$, solution of the Helmholtz equation between two points in space, as [2]

$$G^R(\mathbf{r}_k, \mathbf{r}_s) = \sum_{i=1}^I a_i G(\mathbf{r}_k, \mathbf{r}_i) \tilde{G}(\mathbf{r}_i, \mathbf{r}_s), \quad k = 1, \dots, K. \quad (1)$$

where $G(\mathbf{r}_k, \mathbf{r}_i)$ is the Green function between reflector located at bottom position \mathbf{r}_i and sensor at \mathbf{r}_k , $\tilde{G}(\mathbf{r}_i, \mathbf{r}_s)$ is the bottom incident field at \mathbf{r}_i from the sound source at location \mathbf{r}_s , a_i is the complex amplitude coefficient of the i -th reflector assumed random distributed and finally I is the number of effective reflectors. k , due to shot l is The source-bottom-array geometry defines the contributing reflectors of the bottom spatial grid at each time, as the system moves along. Under certain conditions of reflectors sparsity, bottom discretization over I reflectors allows for direct inversion for the amplitudes a_i which can be termed as a full-field (or matched-field) compressed sensing (CS)-based approach.

¹funded under the EU H2020 research program, contract ICT-645141

B. DSA and compressed sensing

The problem of DSA geometry optimization may be cast as an optimization search that requires defining both the optimization criteria and the parameter search domain. The parameter search domain is clearly set as the three dimensional space coordinates. This coordinate system can not be seen (or defined) independently from the source position and from the physical environmental scenario where the survey takes place, which makes the search itself case dependent.

The approach of compressed sensing (CS) has proven interesting for this purpose since it entails two important aspects: one is that it requires a randomization of the observation matrix and the other is the notion of low coherence, that is directly derived from the observation matrix, and serves as an indicator of the success for the retrieval of the information of the low-rank / sparse process under observation.

The importance of (1) is that it establishes a link between the target and the receiver domain by means of the appropriate Green functions. A full discretization of the sub-bottom into $M = M_1 \times M_2 \times M_3$ samples along a $x \times y \times z$ grid, where only a reduced number of grid points have effective reflectors, allows to cast the inverse problem into a sparse system of equations under the form

$$\mathbf{g} = \mathcal{G}\mathbf{x}, \quad (2)$$

where

- \mathbf{g} is a vector $J \times 1$
- matrix $\mathcal{G} = G(\mathbf{r}_j, \mathbf{r}_m)\bar{G}(\mathbf{r}_m, \mathbf{r}_s)$ is $J \times M$, where the vectors $\mathbf{r}_m; i = 1, \dots, M$ span the sub-bottom target domain, $\mathbf{r}_j; j = 1, \dots, J$ span the sensor space domain, \mathbf{r}_s is the source vector and
- \mathbf{x} is a $M \times 1$ vector that is all zeros but for values $a_i, i = 1, \dots, I$ of effective reflectors.

So, for $I \ll M$, (2) represents a sparse system of equations. Determining an accurate estimate $\hat{\mathbf{x}}$ of the sparse vector \mathbf{x} would allow to obtain an estimate \hat{I} of the number of effective reflectors I as the non zero values of $\hat{\mathbf{x}}$ and, an estimate \hat{a}_i of its relative reflection.

A tractable solution of (2) using a l_1 -norm minimization algorithm will mainly depend on the mutual coherence of matrix \mathcal{G} . Since \mathcal{G} is a matrix that depends on the Green functions of the media between source - bottom - receiver its values should not be modified and there is no low coherence guarantee. The proposed solution allowing to decrease the mutual coherence without changing the observation matrix is based on the randomization of the rows of matrix \mathcal{G} [1]. This is done by observing vector \mathbf{g} through a channel sampling matrix $\tilde{\Phi}$ of dimension $K \times J$, for $K \ll J$, and where each row of $\tilde{\Phi}$ will have a single 1 at a random position among the J columns. Thus we can form the observation \mathbf{y} ,

$$\begin{aligned} \mathbf{y} &= \tilde{\Phi}\mathbf{g}, \\ &= \tilde{\Phi}\mathcal{G}\mathbf{x}, \\ &= \mathbf{A}\mathbf{x} \end{aligned} \quad (3)$$

where now $\mathbf{A} = \tilde{\Phi}\mathcal{G}$, of dimensions $K \times M$ with $K \ll M$ and with $\|\mathbf{x}\|_0 = I^1$, and $I \ll K$, forming a sparse system of

¹the l_0 -norm is used as the number of non-zero values of vector \mathbf{x} .

equations. The mutual coherence $\mu(\mathbf{A})$ is defined as

$$\mu(\mathbf{A}) = \max_{j,k=1,M} \frac{|\langle \mathbf{a}_j, \mathbf{a}_k \rangle|}{\|\mathbf{a}_j\|\|\mathbf{a}_k\|}. \quad (4)$$

There is, however, no guarantee that a solution can be reached through

$$\min_{\mathbf{x} \in \mathbb{R}^M} \|\mathbf{x}\|_1 \quad s.t. \quad \mathbf{A}\mathbf{x} = \mathbf{y} \quad (5)$$

although a solution is attainable with high probability when $\mu(\mathbf{A})$ is low. So, coherence plays an important role in CS and in information bearing sensors in general. An interesting result mentioned in [3], [4] gives the required number of measurements K for a given sparsity level I , bounded by the coherence $\mu(\mathbf{A})$, as

$$K \geq c\mu^2(\mathbf{A})I \log M. \quad (6)$$

where c is some positive constant. It can be easily seen that for moderate coherence, a low number of K measurements 20 to 40, per resolvable layer I may be used, almost independently from the required number of discretization samples. This is the reason why CS is essentially devoted to low coherence measurements, where the "compression gain" is most prominent. The idea behind DSA geometry optimization is to determine the sensor placement that minimizes the mutual coherence $\mu(\mathbf{A})$, of course, conditioned on the operational restrictions imposed by the system constraints and on the a priori knowledge of the environmental conditions of the test site.

III. FOT ARCHITECTURE

A simplified block diagram of the FOT architecture is given in Figure 1. The block boxes are color coded as follows: required inputs to the tool (red), processing algorithms (black) and optional information (light blue). The "best formation" is the expected output given as the source - receiver relative positions and only requires the required inputs (red boxes). If the "true environment" is also given as input, FOT produces the "estimated model" that represents, what would be the estimated sub-bottom if the reality was identical to the true environment using the best formation (or any other specified by the user for comparison).

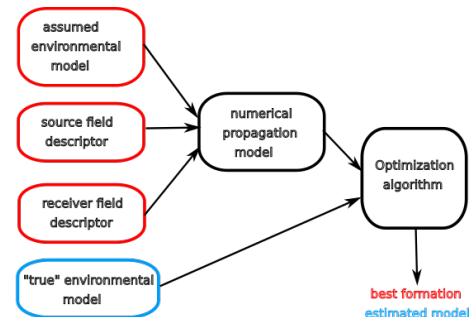


Fig. 1: Formation Optimization Tool overall block diagram: mandatory input information (red), optional information (light blue) and processing algorithms (black).

The aggregation of the environmental and system information is performed through an input file to a well suited acoustic

numerical propagation model, in this case the Ocean Acoustic and Seismic Exploration Synthesis (OASES) [5]. The OASP module will be extensively used in FOT. Input files for these various packages are slightly different but the core information is shown in table I.

Frequency	1000 (Hz)					
Layer	Depth (m)	C_p (m/s)	C_s (m/s)	α_p (dB/ λ)	α_s (dB/ λ)	ρ (Kg/cm ³)
water		1512	0	0	0	1
sed 1	23	1650	150	0.5	2.0	1.8
bottom	24	4750	2350	0.1	0.3	2.5
Source depth	0.3 (m)					
Range min	0 (Km)					
Range max	0.5 (Km)					
Receiver depth	0.3 (m)					
Scan depth max	50 (m)					

TABLE I: Sines’17 canonical scenario OASES model parameters: source frequency, C_p -compressional velocity, C_s -shear velocity, α_p -compressional attenuation, α_s -shear attenuation and ρ -density, and source receiver positioning.

IV. APPLICATION TO SINES PORT

The experiments were carried out in a protected area of the container port of Sines, in the southwest coast of Portugal as shown in the area map of Fig. 2 (a). No digital bathymetry was available for this area, but a close look at the Navionics yacht chart² of Fig. 2 (b) let us know that the area in front of the pier (T shaped structure on the left side of the figure) is mostly flat with depths varying between 22 and 23 meters (white colored contours) in the center.

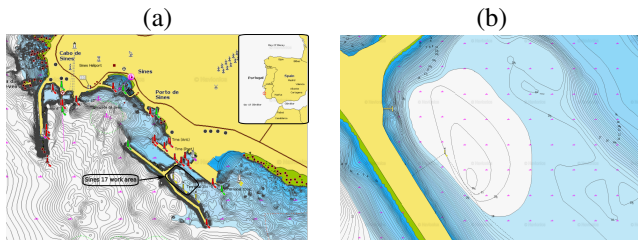


Fig. 2: Sines 2017 experiment: area map with location Sines location in Portugal (insert) and experiment working area in Sines Port (a) and bathymetry as extracted from a Navionics yacht chart (b).

The sound velocity profiles taken in the area are shown in Fig. 3, where the water column tends to be lightly stratified during the day, but remains mostly isotropic with a mean sound speed on the order of 1511 m/s.

Historical data made available from the consortium that built the port of Sines, filtered the idea that the bottom is hard basalt with a very thin sediment layer of probably less than a meter thick with, eventually, eroded areas where basalt patches may surface at the sea bottom.

In WiMUST seismic sources are of sparker type, mounted on small catamaran ASV. Due to the dimensions of the

²<http://www.navionics.com/>

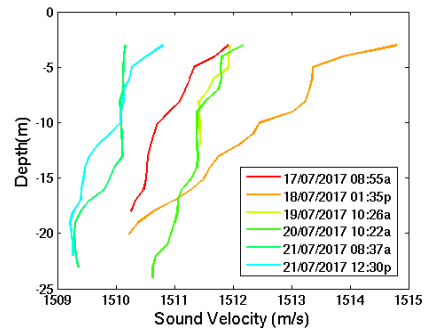


Fig. 3: Sound velocity profiles taken in Sines port during the Sines’17 experiment.

catamarans the horizontal distance between vehicles should be within Xmin/max and Ymin/max in range and cross-range, respectively. The necessary information for source field setup is shown in table II.

Source	type	depth (m)	E (J)	BW (Hz)	Xmin/max (m)	Ymin/max (m)
Delfim	sparker	0.3	300	500-2500	2/50	2/15
Ulisse	sparker	0.3	300	500-2500	2/50	2/15

TABLE II: Source field parameters for Sines’17 experiment.

The receiver field is formed by $R = 2/4/6$ AUVs carrying a streamer with $P = 8$ acoustic sensors (hydrophones) each, so a total of $K = R \times P$ sensors. Minimum range and cross-range distance between vehicles (or between arrays and vehicles) is set to 2 m, while the maximum distance between any vehicle and the pilot ASV is set to 50 m in range and 15 m in cross-range. Vehicle depth min and max values are 0.3 and 5 m, respectively (at least for the Medusa class vehicles). There are two types of vehicles with quite different characteristics from the navigation point of view, but with little impact on the formation design and bottom acoustic information retrieval, since acoustic streamers are identical for all vehicles. The streamers are composed of a neutrally buoyant oil-filled hose with 8×1 m-spaced hydrophones. The acoustic active part of the array is connected to the vehicle through a 2-3 m long cable. Data acquisition is made on a specially designed board physically connected to the vehicle.

Source	type	# ch	d (m)	BW (Hz)	Xmin/max (m)	Ymin/max (m)	Zmin/max(m)
Medusa	auv	8	1	100-5000	2/50	2/15	0.3-5
Folaga	auv	8	1	100-5000	2/50	2/15	-

TABLE III: Receiver field parameters for Sines’17 experiment.

A. Sines’17 best formation prediction

According to the minimum coherence principle set forth in section II-B, conditioned on the environmental and system a priori information, the “best” vehicle formation corresponds to the AUV distribution on a surface grid such that the field coherence of the observation matrix, given by (4), is minimum.

The usage of a Genetic Algorithm (GA) for decreasing the computational load is purely instrumental but necessary when the number of grid points and / or the number of sensors (assets) grows. The number of assets was set to $L = 2$ two sparker sources and $R = 4$ receiving AUVs. According to specifications the position of the two sources was set to minimum 4 m apart and one of the sparkers was 3 m (relative to the direction of survey) behind the other. Several runs were made with different grid coverage and some test results are shown in Fig. 4 for a grid 6 m wide \times 30 m long (a) 6 m wide \times 50 m long (b) 8 m wide \times 50 m long (c) and 12 m wide \times 50 m long (d). This figure shows the sources and

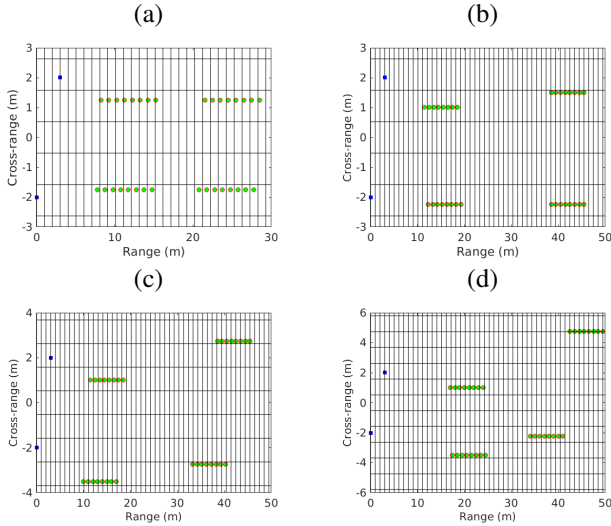


Fig. 4: Sines'17 predicted formations, sources (blue) and receivers (green) for a grid: 6m wide \times 30m long (a) 6m wide \times 50m long (b) 8m wide \times 50m long (c) and 12m wide \times 50m long (d).

the receivers' "optimal" distribution according to the minimum coherence criteria, blue and green filled circles, respectively. The coherence estimate improves as the number of grid points increases, which is merely due to the increased diversity of the field over space. What is not shown in these figures is the actual predicted performance for layer estimation which can be run in parallel by setting a "true" bottom model (blue box in the block diagram of Fig. 1). The chosen "true bottom" model is shown

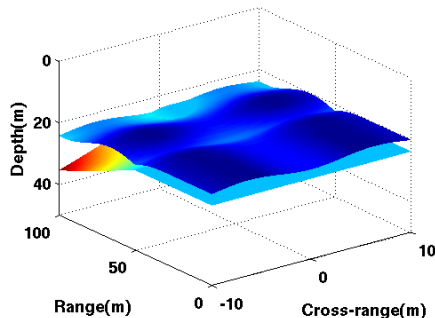


Fig. 5: Sines'17 considered true bottom layering for comparison test purpose.

in Fig. 5 while the estimated sub-bottoms are shown in Fig. 6 for a random distributed geometry and the "best" geometry, in (a) and (b), respectively. In this case the survey system was run over an area of 20 \times 100 m which implies several contiguous passes (lawn-mower style). The improvement obtained at the

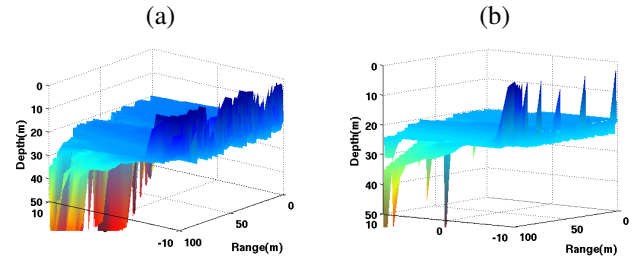


Fig. 6: Sines'17 scenario: estimated bottom for the 6m wide \times 50m long grid case with random geometry (a) and optimized geometry (b).

-10m cross-range border line and at the sub-bottom deepening layer corner ($y=10, x=100$ m) over the random case is clear, when passing from the random to the optimized geometry.

V. CONCLUSION

The low-coherence field is concept is used in this work to develop a formal tool - called Formation Optimization Tool (FOT) - for computing best vehicle formation estimates. FOT is described in detail and is applied to the Sines Port scenario. According to the existing a priori data a series of "best suited" AUV formations was proposed for the Sines'17 but could not be validated at sea. However, assuming a theoretical mismatch model of the assumed environment and using a sparse array algorithm inspired in CS, allowed to assert that the "best suited" array geometries effectively outperformed random generated or regular geometries.

ACKNOWLEDGMENT

This work was funded under H2020 Research program of the European Union under project WiMUST contract ICT-645141.

REFERENCES

- [1] S. Jesus, "Distributed sensor array for bottom inversion," in *IEEE/OES China Ocean Acoustics COA'2016*, Harbin, China, January 2016.
- [2] A. Fannjiang, P. Yann, and T. Strohmer, "Compressed remote sensing of sparse objects," *arXiv:0904.3994*, 2009.
- [3] E. Candès and J. Romberg, "Sparsity and incoherence in compressive sampling," *Inverse Problems*, vol. 23, pp. 969–985, 2007.
- [4] E. Candès and M. Wakin, "An introduction to compressive sampling," *IEEE Signal Processing Magazine*, vol. 25, no. 3, pp. 21–30, March 2008.
- [5] H. Schmidt, *OASES 3.1 - User guide and reference manual*, MIT, March 2011.